Appl. Magn. Reson. 30, 1–XXX (2006)

Applied Magnetic Resonance

CW EPR, Echo-Detected EPR, and Field-Step ELDOR Study of Molecular Motions of Nitroxides in *O*-terphenyl Glass: Dynamical Transition, Dynamical Heterogeneity and β-Relaxation

S. A. Dzuba, E. S. Salnikov, and **L. V. Kulik**

Institute of Chemical Kinetics and Combustion, Novosibirsk, Russian Federation

Received May 15, 2006

Abstract. Continuous-wave electron paramagnetic resonance (CW EPR), echo-detected (ED) EPR, and field-step electron-electron double resonance (FS ELDOR) were simultaneously applied to study molecular motions of nitroxide spin probes of two different types in glassy o-terphenyl. A strong linear temperature dependence of the overall splitting of the CW EPR lineshape was found for nitroxide Tempone and only a weak one for a phenyl-ring containing imidasoline nitroxide. The linear temperature dependence of the splitting is explained within the model of harmonic librations. The assessed libration frequency for Tempone is of the order of $3 \cdot 10^{12}$ rad/s. The observed remarkable difference between two nitroxides is explained by the different strength of interactions between guest and host molecules and by dynamical heterogeneity of the glass. The nonlinear temperature dependence above 250 K is attributed to the onset of anharmonic motion that is postulated in a number of neutron scattering and Mössbauer spectroscopy studies for molecular glasses and proteins (the so-called dynamical transition). Above 245 K also ED EPR spectra change drastically, which may be explained on the same ground. Magnetization transfer was observed in FS ELDOR for nitroxide Tempone, with a time constant around 10^{-5} s. It was found to be almost temperature-independent between 160 K and 265 K and was attributed to the Johari–Goldstein β-relaxation process. For the phenyl-ring containing imidasoline nitroxide this transfer was not observed which may be explained again by the dynamical heterogeneity of the glass and by small effectivity of the β-relaxation process in this case.

1 Introduction

Electron paramagnetic resonance (EPR) of nitroxide spin probes and labels and of other paramagnetic molecules is often used to study orientational molecular dynamics in glassy media. Different approaches in EPR were employed: continuous-wave (CW) EPR [1–4], including high-field CW EPR [5, 6], echo-detected (ED) EPR [7–12], stimulated echo decay [13, 14], field-step electron-electron double resonance (FS ELDOR) [15–20], pulsed two-dimensional EPR [21], and some others. EPR allows addressing the important issues of molecular dynamics

in glasses, such as the mechanism of motion of individual guest molecules, the cooperative nature of motion, temperature dependence of motion, the relation to glass transition, the distribution of correlation times, dynamical heterogeneity and others.

So far, the interrelation of different EPR approaches, as well as their relation to other experimental techniques [dielectric and nuclear magnetic resonance (NMR) relaxation, light and neutron scattering, etc.] is rarely discussed in literature. Moreover, data of different EPR techniques are often interpreted within different motional models: isotropic or anisotropic Brownian motion, jump orientational motion, orientational oscillations (librations), wobbling motion, etc.

In the present work we study nitroxides in a molecular glass of *o*-terphenyl employing simultaneously CW EPR, ED EPR, and FS ELDOR. The goal is to compare results obtained within these different EPR techniques and also with results of other techniques known from literature. *O*-terphenyl can be easily supercooled without crystallization (T_g = 243 K). The dynamics of its molecules was studied by a large variety of different experimental approaches.

Recently, much attention has been attracted to so-called dynamical transition in molecular glasses and biomolecules, which manifests itself as a sharp increase of amplitude of molecular motion above some certain temperature. For proteins this temperature lies between 200 and 230 K. This transition was detected by Mössbauer spectroscopy [22–25] and neutron scattering [25–29]. It is known to affect the physiological function of proteins [24–26]. The manifestation of this phenomenon in EPR was discussed in refs. 4 and 30. It is explored further in the present paper.

2 Experimental

The structures of nitroxides are

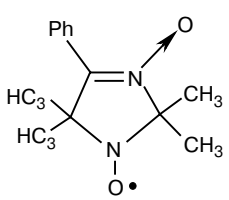

I (phenyl-imidasoline)

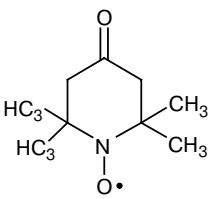

II (Tempone)

Nitroxide I (2,2,5,5-tetramethyl-4-phenyl-3-imidasoline-3-oxide N-oxide or phenyl-imidasoline) was kindly donated by I. A. Grigoryev. Its synthesis is described in ref. 31. Nitroxide II (2,2,6,6-tetramethyl-4-piperidone N-oxide or Tempone) was purchased (Sigma) and purified by recrystallization from hexane. The nitroxide concentration in *o*-terphenyl (Aldrich) was about 10^{-3} M. The samples of liquid o-terphenyl containing dissolved nitroxides were prepared above melt-

ing point and then rapidly frozen. The transparency of the samples was checked before and after measurements to prove that no crystallization had occurred.

Experiments were performed on an X-band Bruker ESP 380E pulsed EPR spectrometer using either a standard Bruker rectangular cavity (CW EPR experiments) or a homebuilt rectangular cavity operating at H_{012} mode (ED EPR). For CW experiments, the operating parameters were chosen to avoid saturation and overmodulation. In pulsed experiments, the cavity was overcoupled to adjust the dead time to 120 ns. Duration of microwave pulses was 32 and 64 ns for $\pi/2$ and π pulses, respectively. ED EPR spectra were taken by scanning magnetic field and keeping constant the time delay τ between pulses.

The experimental approach to study magnetization transfer using rapid field stepping was the same as described in ref. 16. Briefly, a three microwave pulse sequence, π–T–$\pi/2$–τ–π–τ-echo was used. The first pulse is applied at the maximum of EPR spectrum. It serves as a hole-burning pulse, inverting magnetization at the center of the hole. Before application of the second pulse, the resonance magnetic field is shifted to the position of the low-field spectral edge (a 23 G shift). The echo signal serves as a measure of longitudinal magnetization at this field position. The dependence on T then will provide the kinetics of magnetization transfer between the central and the low-field components. All technical details of present equipment for performing field stepping are described in ref. 32.

A Bruker variable-temperature Unit ER 4111VT was used. A Cu–constantan thermocouple was placed in the sample tube to monitor the sample temperature. This setup provided temperature stabilization during the experiment within ± 1.5 K.

3 Results and Discussion

CW EPR. CW EPR spectra of nitroxides consist of three hyperfine structure (hfs) components corresponding to three nitrogen spin projections. At the temperatures of our study (below 280 K) CW EPR spectra are motionally frozen and the line shape only slightly depend on temperature [6]. In the absense of motion the line shape is determined by the anisotropy of hf interaction (hfi) and of g-factor. Figure 1a shows the temperature dependence of the splitting between the two outer peaks. One can see for Tempone a noticeable decrease of the splitting with increasing temperature. The same decrease is known for a number of glass-forming liquids containing soluted nitroxides [1–4]. It was assigned to molecular motions and described within different models of motion: isotropic and anisotropic Brownian diffusion, orientational jumps via arbitrary angles, fast librations, etc. Note however that CW EPR spectra, taken alone, are not critical to the motional model. Moreover, a slight temperature dependence of the apparent hfi parameters may be interpreted as arising from other sources, e.g., from the temperature dependence of the matrix polarity [33]. (In our case, because of the low polarity of the matrix, this effect may be ruled out.) To choose properly the motional model, data from other techniques must be involved.

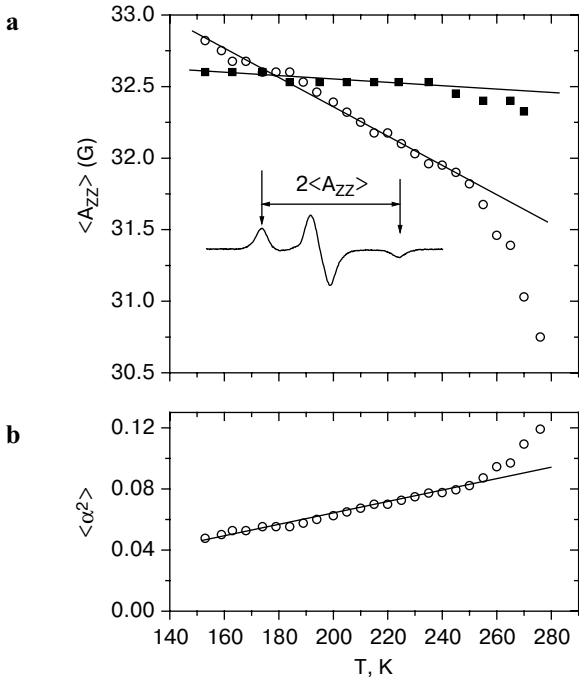

Fig. 1. a temperature dependence of the splitting between two outer peaks (shown in the inset) for phenyl-imidasoline (squares) and Tempone (circles). The straight lines are drawn through points taken below 250 K. **b** Mean-squared amplitudes of angular motion, obtained for Tempone from data (**a**) using Eq. (1).

In our opinion, the models of unrestricted orientational motions such as Brownian diffusion (including uniaxial diffusion) or jump rotations may be certainly ruled out basing on the data available in literature. Experiments with a light-oriented spin probe did not show a change of the orientation of a probe at the temperatures where the temperature dependence of EPR line shape is observed [34]. Single molecule studies of fluorescent probe molecule [35] show that near T_g unrestricted motion occurs only at the second time scale which is many orders of magnitude larger than the time scale when motion manifests itself in EPR ($\sim 10^{-7}$ s). Hole-burning experiments in FS EPR for nitroxides in glasses near T_g did not show any broadening of the localized hole at the timescale of the experiment ($\sim 10^{-5}$ s) [16, 17, 20], which certainly must be expected for unrestricted motion.

Numerical data on ED EPR spectra taken near and above T_g are quantitatively described by the low-amplitude librational model [7–12]. This motion is restricted in the angular space. For fast librational motion (frequency higher than 10^8 rad/s) the CW EPR line shape is determined by the same equations as a solidlike CW EPR spectrum, with the principal hfi and *g*-factor values replaced by their motion-averaged counterparts [4, 12]. The splitting between the two outer

peaks in Fig. 1 corresponds with good accuracy to the $2A_{ZZ}$ value (the molecular Z-axis is perpendicular to the >NO plane). For the uniaxial librations with the motional axis lying in the >NO plane (for the motional axis parallel to the Z-axis anisotropic relaxation is much slower) and with the amplitude α, the motion-averaged $\langle A_{ZZ} \rangle$ value will be

$$\left\langle A_{ZZ} \right\rangle = A_{ZZ}^0 - (A_{ZZ}^0 - A_{\perp}^0)\left\langle \sin^2 \alpha \right\rangle \approx A_{ZZ}^0 - (A_{ZZ}^0 - A_{\perp}^0)\left\langle \alpha^2 \right\rangle, \tag{1}$$

where the superscript denotes data for a motionless molecule. The potential well is symmetric, so that $\langle \alpha \rangle = 0$. For small amplitude of motion one may replace $\langle \sin^2 \alpha \rangle$ by $\langle \alpha^2 \rangle$.

Below 250 K the dependences in Fig. 1 are close to the linear ones. Such a behavior previously has been observed in other CW EPR studies [4, 12]. It was attributed to the manifestation of fast harmonic librations at low temperatures. Indeed, from Eq. (1) it follows that a linear temperature dependence of the hfi constants means that mean-squared amplitude of libration motion, $\langle \alpha^2 \rangle$ also linearly depends on temperature. This behavior is typical for harmonic solids, because in that case

$$\frac{I\Omega^2 \left\langle \alpha^2 \right\rangle}{2} = \frac{kT}{2}, \tag{2}$$

where I is the moment of inertia, Ω is the oscillator frequency, k is the Boltzmann constant.

Such behavior indeed was observed in molecular glasses in numerical neutron scattering and Mössbauer absorption studies [22–29], mean-squared amplitude of vibrational displacement.

Figure 1b presents $\langle \alpha^2 \rangle$ obtained for Tempone from data of Fig. 1a employing Eq. (1). A_{ZZ}^0 was obtained by extrapolating the straight line to zero temperature (neglecting so by quantum effects in oscillating motion). Taking for the Tempone molecule $I \sim 5 \cdot 10^{-38}$ g $\cdot$ cm^2, from Fig. 1b and Eq. (2) we obtain $\Omega \sim 3 \cdot 10^{12}$ rad/s.

Above 250 K a departure from the linear dependence is seen in Fig. 1b. This could be attributed to the onset of the large-amplitude anharmonic motions known from neutron scattering data, and which for pure *o*-terphenyl occurs also near 250 K [27, 28].

For phenyl-imidasoline the observed slope of the dependence is very small (Fig. 1a), which may be readily interpreted as a result of a slower motion in that case. Note that EPR data reported earlier [6] also have showen that Tempone in *o*-terphenyl moves much faster than nitroxides having larger size. The remarkable difference between two nitroxides may be explained by taking into account that the molecular structure of phenyl-imidasoline resembles a little bit that of the host *o*-terphenyl molecule (phenyl ring is also present, and the other ring contains p-electrons). Moreover, we have found that a crystalline state of *o*-terphenyl with embedded phenyl-imidasoline may be easily prepared, which also

supports this closeness (while Tempone was found from EPR spectra to aggregate in a separate phase). So one may suppose that intermolecular interactions between guest and host molecules via their p-electrons may retard motion in the case of phenyl-imidasoline.

This retardation of motion may result in that the amplitude and/or frequency of motion will become smaller. The smaller amplitude in turn will result in weaker influence of motion on the A_{ZZ} value. The smaller frequency may result in incomplete averaging of A_{ZZ}, so that Eq. (1) will not be valid (this will indeed occur if $\Omega < 10^8$ rad/s). From data in Fig. 1a it is impossible to decide which of the above reasons is responsible for the weak temperature dependence of $\langle A_{ZZ} \rangle$ for phenyl-imidasoline. Therefore, it impossible to calculate $\langle \alpha^2 \rangle$ for this case.

So, phenyl-imidasoline probably is involved in cooperative motion with surrounding molecules while Tempone moves freely. This finding additionally supports the concept of dynamical heterogeneity of molecular glasses [36, 37]. It looks like that Tempone and phenyl-imidasoline select the regions of fast and slow motions, respectively.

ED EPR. Echo-detected EPR spectra at different temperatures for both nitroxides are given in Fig. 2. To exclude all isotropic relaxation processes which are expected to be field-independent, spectra are normalized to the same value at the field position corresponding to the maximum amplitude. One can see that below 245 K spectra do not depend on temperature. Above this temperature, remarkable temperature dependence takes place, for both nitroxides.

To assess the intensity of motion at different temperatures, we use the relative intensity at the spectral positions where the effect is most pronounced – see insert in Fig. 2. One can see that the onset of ED EPR line shape temperature dependence starts near 250 K.

The ED EPR line shape dependence on τ at fixed temperature (260 K) is presented in Fig. 3. Spectra are refined from the influence of so-called instantaneous diffusion that arises from spin-spin dipolar interaction according to the procedure proposed in [38], where this influence is taken into account by measurement at low temperature (245 K) where temperature dependence is frozen. In Fig. 3 also for comparison are given ED EPR spectra at 245 K.

Both Figs. 2 and 3 show that the broader hfs component, the faster relaxation is. As different spectral positions are related with different nitroxide orientations relative to the external magnetic field, a broader component corresponds to a larger anisotropy. Reorientations of nitroxide molecule induce stochastic fluctuations of the Larmor frequency, which lead to transverse relaxation and which is faster for a larger anisotropy. Therefore the observed changes of the line shape may be explained by orientational motion.

Note the different character of the temperature and τ dependences for phenyl-imidasoline and Tempone (Figs. 2 and 3). For phenyl-imidasoline relaxation is remarkably slower at the field positions corresponding to the canonical orientations of nitroxide (the outer spectral edges correspond to the parallel orientation of nitroxide Z molecular axis respectively to the external magnetic field)

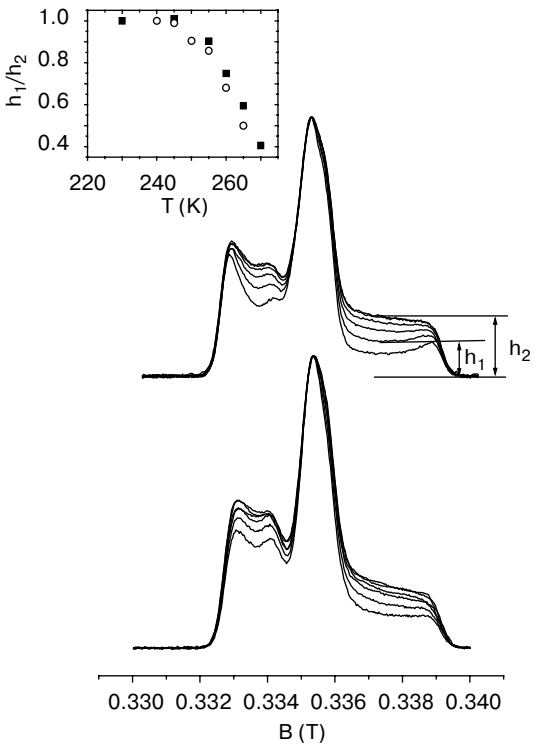

Fig. 2. ED EPR spectra for phenyl-imidasoline (top) and Tempone (bottom), taken at the same time separation $\tau = 200$ ns, at different temperatures. Spectra are normalized to the same amplitude at the field position corresponding to the maximum of the spectrum. Temperatures are 230, 245, 255, 260, 265 and 270 K (top) and 240, 245, 250, 255, 260, 265 K (bottom), the intensities in the shoulders monotonically decrease with temperature increase. This decrease is depicted quantitatively in the insert, where squares refer to phenyl-imidasoline and circles to Tempone (unity at the vertical axis cor responds to the signal taken at 230 K) .

while for Tempone within one component relaxation is approximately field-independent.

This difference may be explained by different amplitudes of motion. If the molecule performs a restricted orientational motion with small amplitude, Larmor frequency fluctuations are larger for the intermediate field positions in the spectrum, between those corresponding to the canonical orientations [8, 12]. This results in faster relaxation and that is just what is observed for phenyl-imidasoline (Figs. 2 and 3). For Tempone motional amplitudes are larger (see Fig. 1b), so the Larmor frequency fluctuations are not sensitive to the position in the spectrum (but they still depend on the hfs component).

Note that in CW EPR (Fig. 1) spectral changes are seen not only above 250 K, but also below this temperature. The explanation of this difference with ED EPR may be given as following [30]. Fast harmonic motion will average A_{ZZ}

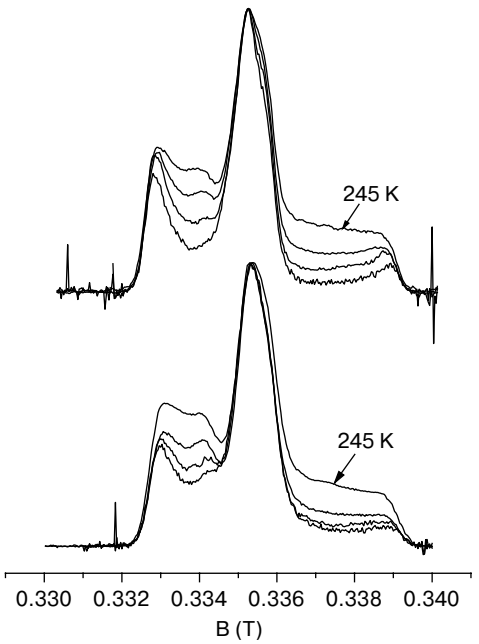

Fig. 3. Same as shown in Fig. 2, for fixed temperature (260 K) and varying τ (200, 400 and 600 ns, intensities in the shoulders monotonically decrease with τ increase). For comparison, a spectrum is given for 245 K, where motional effects are frozen ($\tau = 200$ ns). Spectra are refined from the influence of the process of instantaneous diffusion on the line shape (see text).

and produce temperature dependence in CW EPR. ED EPR depends on anisotropic relaxation that is determined by the spectral density. For fast harmonic motion it is $\langle \alpha^2 \rangle f / \Omega^2$, where f is the friction coefficient [12]. This value may be very small for high frequency Ω.

For anharmonic motion the spectral density may be assessed in the following way. The equation for angular motion for free oscillator may be written as

$$I\ddot{\alpha} + I\Omega^2\alpha - I\Omega^2 \frac{\alpha^2}{\alpha_0} = 0,$$

where α_0 is the parameter of anharmonicity. In the case of small anharmonicity, $\langle \alpha^2 \rangle \ll \alpha_0^2$, the solution will be $\alpha = A\cos\Omega t + \delta$, where A is the amplitude and δ is a small additive, $|\delta| \ll A$. Note that $0\langle \alpha^2 \rangle \approx A^2/2$. For δ the approximate equation is valid:

$$\ddot{\delta} + \Omega^2\delta \approx \Omega^2 \frac{A^2}{\alpha_0} \cos^2 \Omega t.$$

The solution of this equation

$$\delta = \frac{A^2}{2\alpha_0} - \frac{A^2}{6\alpha_0}\cos 2\Omega t$$

contains a nonoscillating additive, which results in the appearance of a nonzero value of $\langle\alpha\rangle$, $\langle\alpha\rangle \approx \langle\alpha^2\rangle/\alpha_0$. Under the influence of thermal stochastic perturbations the $\langle\alpha^2\rangle$ value for a given oscillator will fluctuate (fluctuations of energy) producing the appearance of the spectral density equal to $(\langle\alpha^2\rangle^2/\alpha_0)\tau_c$, where τ_c is the correlation time for energy fluctuations. As this spectral density does not contain Ω in the denominator, the anharmonic librational motion may produce spin relaxation which is much faster than that induced by harmonic motion.

Note that the ED EPR line shape simulated for this model must be exactly the same as that for the model of fast stochastic librational motion, which was employed in a number of previous studies [10–12] (only the spectral density is different, it is $\langle\alpha^2\rangle\tau_c$ for stochastic motion).

The same result, the manifestation of motion at low temperatures in CW EPR and small effects in ED EPR, was obtained in ref. 30 for nitroxides dissolved in glassy glycerol.

There could be two different reasons why anharmonic motion appears with increasing temperature. First, it is because of $\langle\alpha^2\rangle$ increases with temperature, in the temperature-independent anharmonic energy potential. Second, the potential may become anharmonic with temperature increasing (in other words, α_0 becomes smaller). In our opinion, the latter explanation is preferable, because the former one cannot explain the very sharp temperature dependence observed in experiment (see Fig. 2).

We also studied the ED EPR line shape for crystalline samples containing phenyl-imidasoline and found that it depends neither on temperature in the studied temperature range from 200 to 265 K nor on the τ value in the studied interval from 200 ns till 1200 ns (data not given). This result confirms once more that molecular librations seen in ED EPR are an exclusive property of the glassy state. Note that neutron scattering shows the presence of harmonic motion for both crystalline and amorphous samples, while anharmonic motion is seen only in the amorphous state [28]. So the obtained result confirms once more that ED EPR is sensitive to anharmonic motion only.

Simulation of ED EPR spectra. Simulations were performed for a model of purely stochastic librations (fast wobbling) described in ref. 12. Principal values of the magnetic tensors and individual line widths were assessed from ED EPR spectra taken below 245 K. The motional model used in simulations assumes simultaneous and independent librational motions around three perpendicular axes corresponding to the principal axes of the nitroxide magnetic tensor. In this model the net relaxation is given by the product of the three independent relaxations. This model of simultaneous motion was found to agree better with our experiment. Only a single fitting parameter is used in the simulation: the

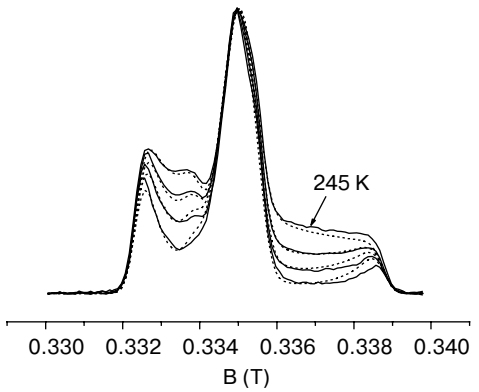

Fig. 4. Same as in Fig. 3 for phenyl-imidasoline, at temperature 265 K (solid lines). Dotted lines present computer simulation for the model of stochastic molecular librations. Simulations employ only single fitting parameter, $\tau_c\langle\alpha^2\rangle$, with the found best-fitted value of 1.2 10^{-12} rad^{2}s. The spectrum taken at 245 K was simulated with $\tau = 0$.

spectral density. The result of this simulation is given in Fig. 4. One can see that this model gives an almost quantitative description of the experimental ED EPR spectra for phenyl-imidasoline. The best-fit value of the spectral density for simulations shown in Fig. 4 was found to be $1.2 \cdot 10^{-12}$ rad^{2}s.

The used low-amplitude librational model did not allow us to simulate with the same quality ED EPR spectra for Tempone shown in Fig. 3. The explanation could be that the amplitude of motion is so high that the model is not valid. We tried the model which assumes angular jumps between two fixed positions [38], with a rectangular distribution of jump angles, which may be large. The satisfactory agreement has been achieved for different sets of the distribution width and times τ_c (data not shown).

It is of interest to note that experimental points in the inset in Fig. 2 for both nitroxides are close. The analogous result showing the independence of anisotropic relaxation of the nitroxide structure was obtained previously for a number of other glassy systems studied by ED EPR [39] (at 77 K). The reason for this needs further investigation.

FS ELDOR. The kinetics of magnetization transfer (MT) from the central component to the low-field shoulder (see Experimental) is shown in Fig. 5. One can see a remarkable MT effect at different temperatures for Tempone. MT manifests itself as an initial decrease of the signal, then the signal restores due to spin-lattice relaxation.

Only a negligible effect is seen for phenyl-imidasoline. The initial decrease is absent in this case. Experiments with phenyl-imidasoline embedded into a crystalline *o*-terphenyl state gave the same kinetics (data not shown). MT normally is related with molecular motion [15–20]. As molecular motion is expected to depend substantially on the physical phase state of the matrix, we conclude that time kinetics seen in Fig. 5 for phenyl-imidasoline presents only longitudinal

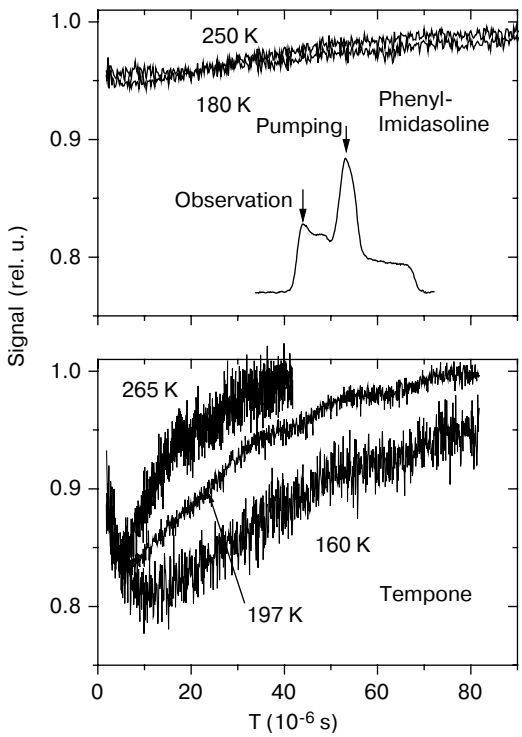

Fig. 5. Kinetics of magnetization transfer between the pumped central component (see insert) and the detected low-field shoulder (unity at the vertical axis corresponds to equilibrium). Top: phenyl-imidasoline, bottom: Tempone.

relaxation after hole-burning, with hole edges attaining the spectral shoulder where the observation is performed. So, it looks that no MT transfer at all takes place for phenyl-imidasoline.

Note that the initial decrease of the signal for Tempone is almost temperature-independent. This is to be compared with the data of CW EPR (Fig. 1) and ED EPR (Fig. 2), where the temperature dependences are very remarkable. Another point is that motional effects in ED EPR disappear below 250 K, while MT is seen even at 160 K (Tempone). It is likely therefore that MT is not related directly with molecular librations which manifest itself in CW EPR and ED EPR. The time scale of MT (10^{-5} s) and its weak temperature dependence prompts us to suggest that it is induced by the well-known Johari–Goldstein β-relaxation process [40, 41], as it was assumed in some earlier works [20].

This assumption also allows explaining the absence of MT for phenyl-imidasoline. The mentioned above closeness of molecular structures of phenyl-imidasoline and of host *o*-terphenyl may result that phenyl-imidasoline follows β-relaxation of the host matrix. Recent studies of dielectric β-relaxation for pure *o*-terphenyl and *o*-terphenyl with dipolar solutes [42] have shown that for o-

terphenyl with solutes β-relaxation is much more intensive than for pure host matrix (even taking into account the difference in dipolar moments).

The found remarkably different MT effect for two nitroxides again supports the concept of dynamical heterogeneity of glasses.

4 Conclusions

The temperature dependence of the CW EPR line shape of nitroxides in *o*-terphenyl glass may be explained within the model of fast molecular librations which are harmonic below 250 K and anharmonic above this temperature. The temperature dependence of the mean-squared amplitude $\langle \alpha^2 \rangle$ obtained with CW EPR (Fig. 1b) very closely resembles numerical data on the neutron and Mössbauer absorption [22–29] where the harmonic-anharmonic transition is proposed for the mean-squared amplitude of vibrational displacement $\langle r^2 \rangle$.

Motional effects in ED EPR spectra clearly appear above 245 K (Fig. 2). For the model of low-amplitude librational motion a quantitative and unambiguous theoretical description of ED EPR spectra may be achieved (Fig. 4). The time scale where neutron scattering is sensitive to motion (10^{-14}–10^{-9} s) is in agreement with that for CW EPR spectra ($<10^{-8}$ s). Furthermore, the known $\langle r^2 \rangle$ value, ~0.01–0.02 nm^2 near dynamical transition [27, 28], is in agreement with the estimation (Fig. 1b) of $\langle \alpha^2 \rangle \sim 0.1$ rad^2 (having in mind that the size of a molecule is around 0.1 nm). Therefore, we conclude that CW and ED EPR data and neutron scattering data very likely reflect the same type of motion. This type seems to be a universal feature of glassy media.

Harmonic motion according to the results of this work only weakly influences ED EPR line shapes. It may however manifest itself if isotropic relaxation is slow. The examples are Fremy's salt in glycerol (the absence of methyl groups makes relaxation slower) [12, 30], or different systems studied in ref. 29 at 77 K (isotropic relaxation becomes slower because of low temperature). The other opportunity to observe the harmonic motion is provided by the extremely high sensitivity to the frequency fluctuations attained in high field–high frequency ED EPR [11].

The librational frequency assessed in this work for Tempone from CW EPR, $\sim 3 \cdot 10^{12}$ rad^2/s ($\sim$16 cm^{-1}), corresponds to the typical frequency of the so-called boson peak (15–40 cm^{-1}) found for glassy materials in the low-frequency region of Raman scattering spectra [45, 46]. Probably this implies the same physical background in these two spectroscopic techniques.

Magnetization transfer observed in FS ELDOR for Tempone most probably is related with well-known Johari–Goldstein β-relaxation process [39, 40]. Therefore, this experimental approach may be used as an additional tool to study this universal but still unclear relaxation process.

Manifestation of motion is found to be remarkably different for two nitroxides studied in this work, in all the experimental approaches used. This may be explained by different interactions between guest and host molecules. Phenyl-imi-

dasoline has a phenyl group like host molecules have while Tempone has not. Therefore, phenyl-imidasoline probably is involved in cooperative motion with surrounding molecule while Tempone moves freely in some voids probably existing in glassy media. These findings additionally supports the concept of dynamical heterogeneity of molecular glasses [36, 37].

Acknowledgments

S.A.D. recollects with pleasure discussions with Kev Salikhov who many years ago stimulated him to apply pulsed EPR to study molecular motions, and discussions with Klaus Möbius who encouraged his activity in the field of ED EPR application to molecular librations. This work was supported by Russian Foundation for Basic Research 04-03-32211, by FASI Grant 6271.2006.3 and by the Siberian Branch of the Russian Academy of Sciences (project 50).

References

1. Hwang J.S., Mason R.P., Hwang L.-P., Freed J.H.: J. Phys. Chem. **79**, 489 (1975)
2. Spielberg J.I., Gelerinter E. J.: Chem. Phys. **77**, 2159 (1982); Phys. Rev. B. **30**, 2319 (1984)
3. Ohta N., Kuwata K.: J. Chem. Phys. **82**, 3420 (1985)
4. Paschenko S.V., Toropov Yu.V., Dzuba S.A., Tsvetkov Yu.D., Vorobiev A.Kh.: J. Chem. Phys. **110**, 8150–8154 (1999)
5. Poluektov O.G., Grinberg O.Y., Dubinskii A.A., Lukyanenko L.V., Lebedev Y.S.: Russ. J. Phys. Chem. **62**, 1067–1070 (1988)
6. Earle K.A., Moscicki J.K., Polimeno A., Freed J.H.: J. Chem. Phys. **106**, 9996 (1997)
7. Millhauser G.L., Freed J.H.: J. Chem. Phys. **81**, 37 (1984)
8. Dzuba S.A., Tsvetkov Yu.D., Maryasov A.G.: Chem. Phys. Lett. **188**, 217 (1992)
9. Konda R., Du J.L., Eaton S.S., Eaton G..R.: Appl. Magn. Reson. **7**, 185 (1994)
10. Dzuba S.A.: Phys. Lett. A **213**, 77 (1996)
11. Rohrer M., Gast P., Möbius K., Prisner T.F.: Chem. Phys. Lett. **259**, 523 (1996)
12. Kirilina E.P., Dzuba S.A., Maryasov A.G., Tsvetkov Yu.D.: Appl. Magn. Reson. **21**, 203 (2001)
13. Leporini D., Schädler V., Wiesener U., Spiess H.W., Jeschke.G.: J. Chem. Phys. **119**, 11829 (2003)
14. Dzuba S.A., Kirilina E.P., Salnikov E.S., Kulik L.V. : J. Chem. Phys. **122** (2004)
15. Dzuba S.A., Tsvetkov Yu.D.: Khim. Fizika **1**, 1197 (1982)
16. Dzuba S.A., Maryasov A.G., Salikhov K.M., Tsvetkov Yu.D.: J. Magn. Reson. **58**, 95 (1984)
17. Dzuba S.A.,Tsvetkov Yu.D.: Chem. Phys. **120**, 291 (1988)
18. Dubinskii A.A., Maresh G.G., Spiess H.W.: J. Chem. Phys. **100**, 2473 (1994)
19. Saalmueller J.W., Long H.W., Maresh G.G., Spiess H.W.: J. Magn. Reson. A **117**, 193–208 (1995)
20. Dzuba S.A., Tsvetkov Yu.D.: J. Struct. Chem. **28**, 343 (1987)
21. Saxena S., Freed J.H.: J. Phys. Chem. **101**, 7998 (1997)
22. Parak F., Frolov E.N., Mössbauer R.L., Goldanskii V.I.: J. Mol. Biol. **145**, 825–833 (1981)
23. Nienhaus G.U., Frauenfelder H., Parak F., Parak F.: Phys. Rev. B **43**, 3345–3350 (1991)
24. Parak F.G.: Current Opinion Struct. Biol. **13**, 552 (2003)
25. Cordone L., Cottone G., Giuffrida S., Palazzo G., Venturol G.i, Viappiani C.: Biochim. Biophys. Acta **1749**, 252 (2005)
26. Gabel F., Bicout D., Lehnert U., Tehei M., Weik M., Zaccai G.: Quart. Rev. Biophys. **35**, 327–367 (2002)
27. Petry W., Bartsch E., Fujara F., Kiebel M., Sillescu H., Farago B.Z.: Phys. B Condensed Matter **83**, 175–184 (1991)

28. Tölle A., Zimmermann H., Fujara F., Petry W., Schmidt W., Schober, Wuttke J.: Eur. Phys. J. B **16**, 73–80 (2000)
29. Galiskan G., Briber R.M., Thirumalai D., Garein-Sakai V., Woodson S.A., Sokolov A.P.: J. Am. Chem. Soc. **128**, 32–53 (2006)
30. Dzuba S.A., Kirilina E.R., Salnikov E.S.: J. Chem. Phys. **125**, 054502 (2006)
31. Volodarsky L.B., ed.: Imidazoline Nitroxides: Synthesis Properties, vol. 1. Boca Raton, Fla.: CRC Press 1988.
32. Kulik L.V., Grishin Yu. A., Dzuba S.A., Grigoryev I.A., Klyatskaya S.V., Vasilevsky S.F. Tsvetkov Yu.D.: J. Magn. Reson. **157**, 61–68 (2002)
33. Steinhoff H.-J.: J. Biochem. Biophys. Meth. **17**, 237–248 (1988)
34. Vorobiev A.K., Gurman V.S., Klimenko T.A.: Phys. Chem. Chem. Phys. **2**, 379 (2000)
35. Deschenes L.A., Van den Bout D.A.: J. Phys. Chem. B **106**, 11438–11445 (2002)
36. Ediger M.D.: Annu. Rev. Phys. Chem. **51**, 99–128 (2000)
37. Sillescu H., Böhmer R., Diezemann G., Hinze G.: J. Noncryst. Solids **307**–**310**, 16–23 (2002)
38. Erilov D.A., Bartucci R., Guzzi R., Marsh D., Dzuba S.A., Sportelli L.: J. Phys. Chem. B **108**, 4501 (2004)
39. Kirilina E.P., Grigoriev I.A., Dzuba S.A.: J. Chem. Phys. **121**, 12465–12471 (2004)
40. Johari G.P., Goldstein M.: J. Chem. Phys. **53**, 2372 (1970)
41. Johari J.P.: Ann. N.Y. Acad. Sci. **279**, 117 (1976)
42. Shahin Md., Murthy S.S.N.: J. Chem. Phys. **122**, 014507 (2005)
43. Buitink J., Dzuba S.A., Hoekstra F.A., Tsvetkov Yu.D.: J. Magn. Reson. **142**, 364–368 (2000)
44. Erilov D.A., Bartucci R., Guzzi R., Marsh D., Dzuba S.A., Sportelli L.: Biophys. J. **87**, 3873–3881 (2004)
45. Surovtsev N.V., Sokolov A.P.: Phys. Rev. B **66**, 054205 (2002)
46. Duval E., Mermet A., Surovtsev N.V., Dianoux A.J.: J. Noncryst. Solids **235**, 203–207 (1998)

Authors' addres: Sergei A. Dzuba, Institute of Chemical Kinetics and Combustion, Russian Academy of Sciences, Institutskaya ulitsa 3, 630090 Novosibirsk, Russian Federation
E-mail: dzuba@ns.kinetics.nsc.ru